Clast size, void space, and degree of contortion in spatter piles at Craters of the moon: Implications for eruptions conditions of lunar basalts

Erika Rader[1], Jennifer Heldmann[1], Robert Wysocki[2], and the FINESSE team

[1]NASA Ames Research Center [2]Syracuse University

Spatter pinpoints the intercept of initial temp, accumulation rate, and cooling rate of volcanic deposits

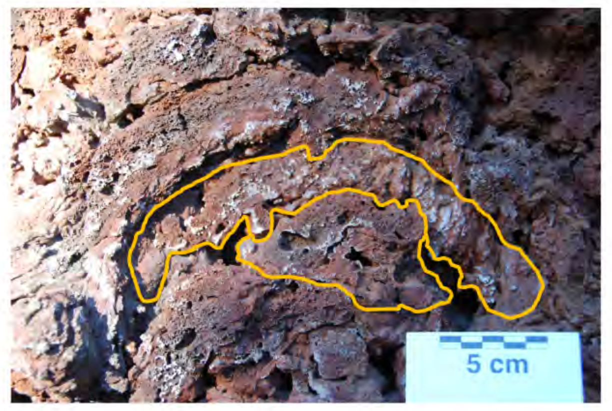

Figure 1. Fluid spatter clasts draped over each other to the right illustrate the partially molten/partially solid nature of lava. Spatter clasts cool upon ejection from the vent and form a more rigid glassy rind that holds the clast's shape. Upon landing, clasts with enough remnant heat can anneal together creating a fused spatter deposit with a higher angle of repose than a cinder cone.

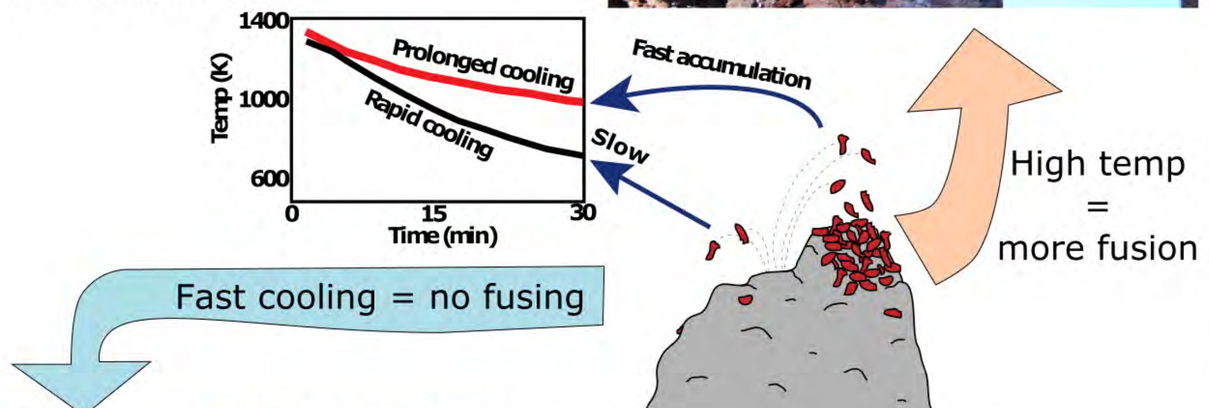

Figure 2. A cross-section of an outcrop comprised of cinder is pictured at left. The clasts were cooled so quickly, they froze in the air before landing. The casts still had some accumulated heat, however, since they oxidized to a red color throughout the clast. The variety of pyroclast morphologies at COTM could be due, in part, to the rate of accumulation of material, which will influence the cooling rate of the deposit.

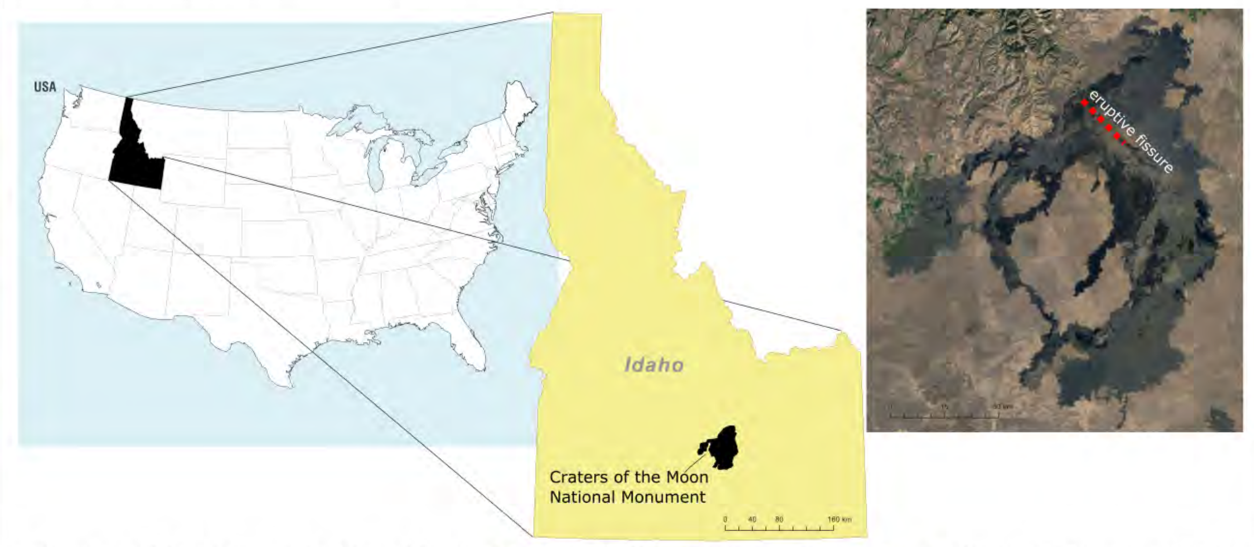

Figure 3. Craters of the Moon National Monument is a lava flow field located in Southern Idaho. It erupted ~30 km^3 of lavas and pyroclasts between 15,000-2,000 years ago (Kuntz et al. 1986). Material is predominantly mafic but SiO_2 can range from 44-65% (Hughes et al. 1999). For this project, spatter outcrops occurred along the eruptive fissure known as the Great Rift.

The diversity of spatter morphology at COTM

Figure 4. A spatter mound at left exhibits typical exterior morphology of spatter deposits. Namely, steep sides, lumpy texture, and irregular distribution of void spaces throughout the outcrop. Fresh spatter is easily distinguishable from lava or scoria because of these features.

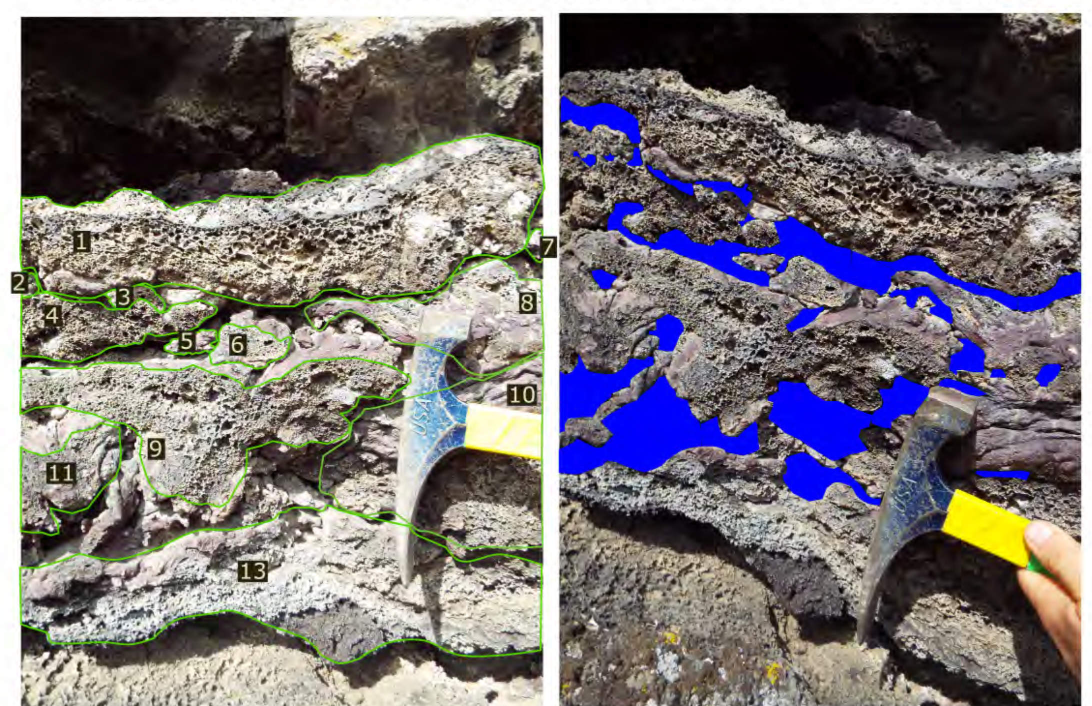

Figure 5. A cross section of a spatter outcrop showing the outlines of individual clasts (bottom left) and the void spaces between clasts (bottom right). The team measured perimeter, thickness, length, rind thickness, and vesicle size in the rind and in the core of each clast in an outcrop. From this data, a large range in spatter textures was found at Craters of the Moon N.M.

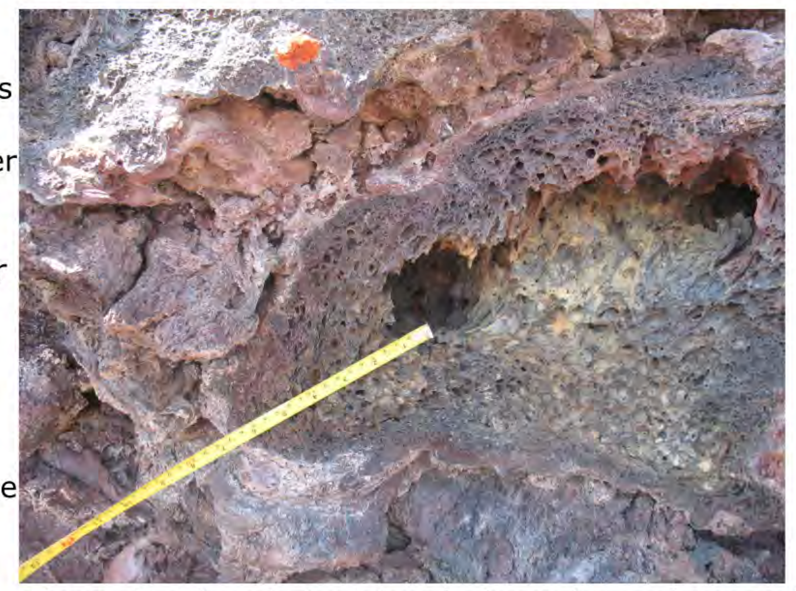

Figure 7. The clast pictured above has a large void space in the core of the clast from vesicle coalescence. The rind contains significantly smaller vesicles and has, proportionally, more glassy material. Despite the large mass of the clast which dictates how much heat is introduced to the system, the layer of scoria above it was unfused, indicating there was significant time between the deposition of each component.

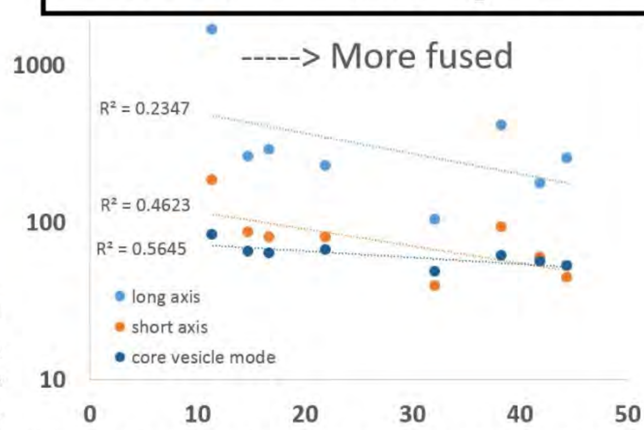

Figure 9. A plot of three variables that have a moderate trend related to degree of fusion (X axis). As amount of connectedness increases, clast axes and mode of vesicles in the core decrease. This suggests that hotter spatter piles were made up of smaller clasts and could not expand as readily at COTM, possibly from rapid accumulation of surrounding clasts.

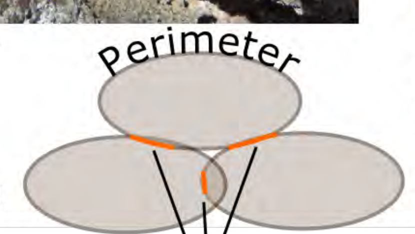

Figure 6. The goal of this physical description of spatter deposits is to find characteristics that correlate to overall temperature. The final characteristic measured was the 'degree of connectedness' which was calculated by dividing the length of the perimeter fused to other clasts by the total perimeter, as illustrated to the right.

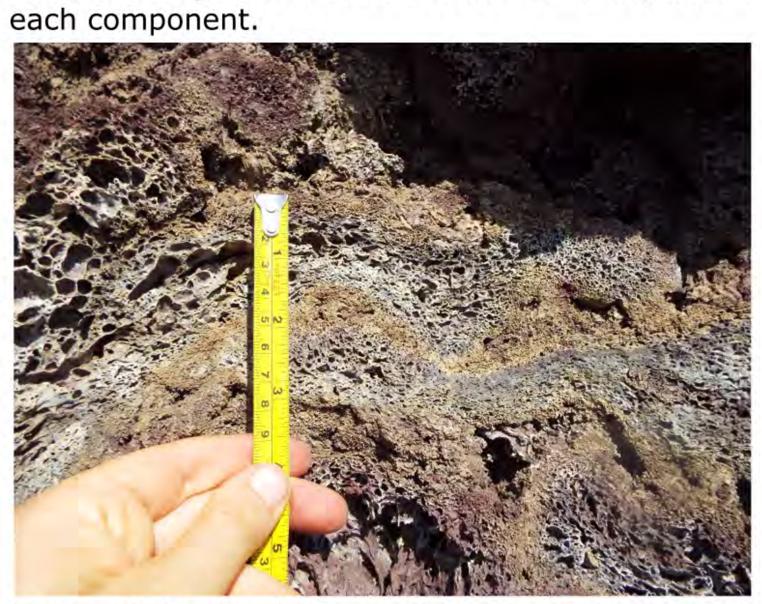

Figure 8. Some clasts exhibited high degrees of connectedness, such as the ones above. The yellow dense material in between the more vesiculated core at about 5 cm on the scale is the fused area between the two clasts. These outcrops had higher degrees of connectedness and are interpreted to be emplaced at a higher temperature.

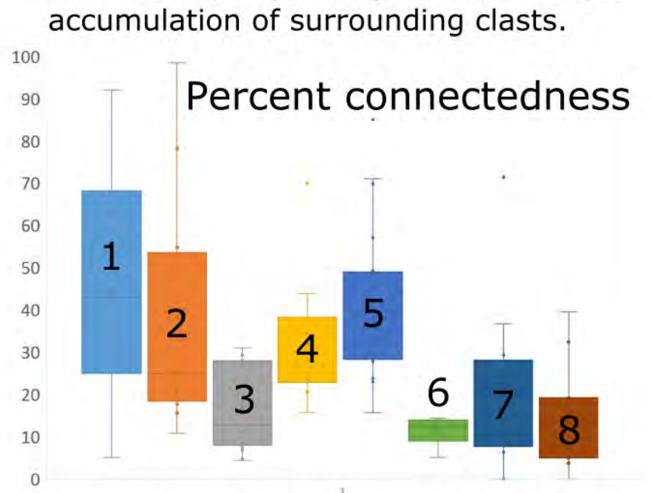

Figure 10. A box and whisker diagram showing the range of connectedness in each outcrop. Some outcrops have a wide range of connectedness in clasts (like 1 and 2) while others are fairly narrow (4,6).

Conclusions:

1. Spatter only forms in a narrow range of eruptive conditions so its presence can signal quantifiable thermal baselines.

2. Experiments on basalt (51 wt. SiO_2%) show that a minimum temp. of 775°C must be held for 30 min to achieve any annealing.

3. Experiments over predict cooling while current numerical modeling under predicts cooling. Lunar spatter may be difficult to form due to longer flight times of clasts and no heat loss by convection.

Do experimental spatter clasts reflect nature?

Figure 11. Experimental spatter clasts are constructed with the furnace at Syracuse University (A). A small volume of molten basalt is poured into a metal trough, which is then manipulated to form a clast (B). The clasts are stacked with thermocouples (C) at each connection and allowed to cool before being deconstructed. SU Lava Project website: www.lavaproject.syr.edu

Figure 12. An experimental spatter pile sits with thermocouple probes extruding from the junctions between clasts on the left. After cooling, the piles are split apart for evaluation. One such evaluation is the percentage of surface area that was fused between the clasts, as seen on the right. Other measurements require clasts to be broken in half, like the size of vesicles and the thickness of the quench rind.

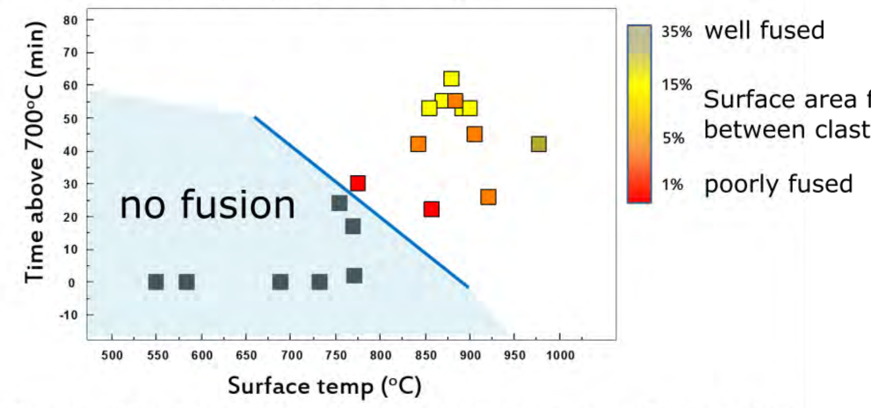

Figure 13. The minimum conditions for fusing between the spatter clasts at SU is shown above on a diagram that compares the surface temperature of the clast just before placement and the time spent above the glass transition temperature (below which no fusion can occur). Starting material has 51 wt. % SiO_2 and ~2.5 NaO + K_2O wt. %. Clasts had to be at least 775°C and stay above 700°C for 30 minutes.

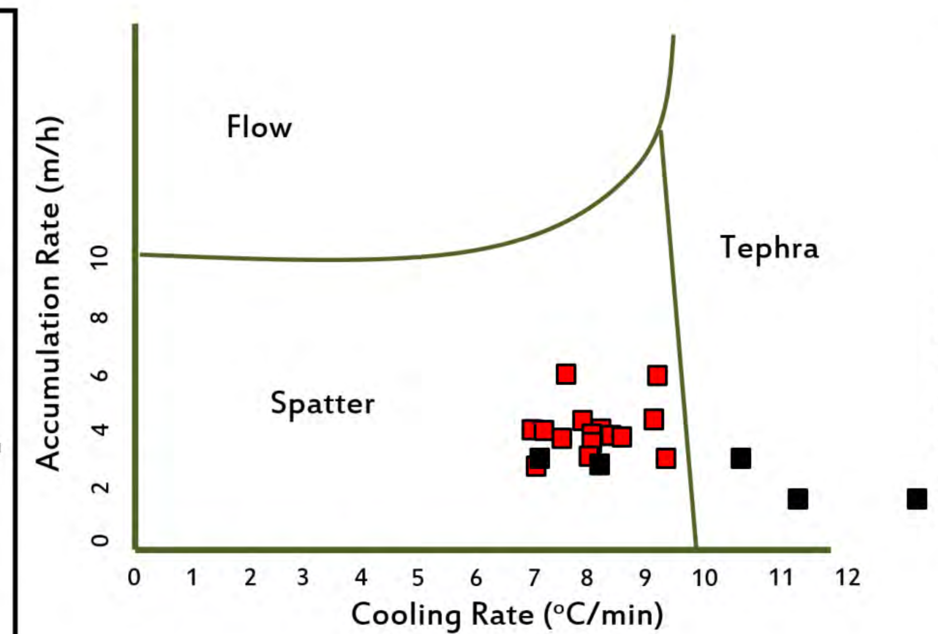

Figure 14. A morphology regime diagram of basaltic pyroclastic deposits so which cooling rates of experimental spatter piles are associated with no fusion (black squares) and therefore plot in the scoria field regardless of the accumulation rates. The boundary between spatter and clastogenic flow (lava) was not found experimentally this project, but an observation was made by Sumner (1998) at a fountain-fed lava flow in Japan. The several black squares that overlap with the red squares (fused spatter clasts), despite lower cooling rates, did not have a high enough starting temperature to anneal to one another. With more work, this diagram will allow field mappers to quantify the cooling and accumulation rates of volcanic terrains.

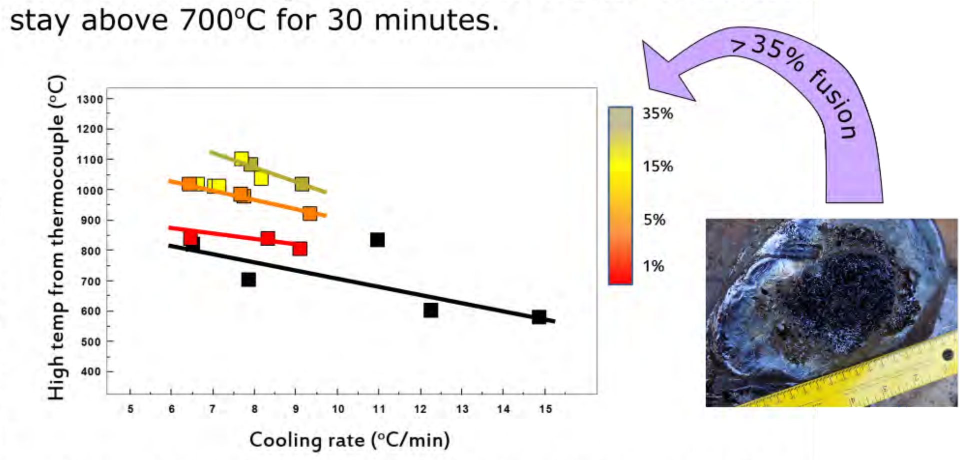

Figure 15. The amount of fusion between clasts seems to be majorly affected by the highest temperature experienced by the weld. For spatter clasts, this indicates the aerial travel time is very important, as the amount of cooling during flight will dictate the high temperature of the deposit.

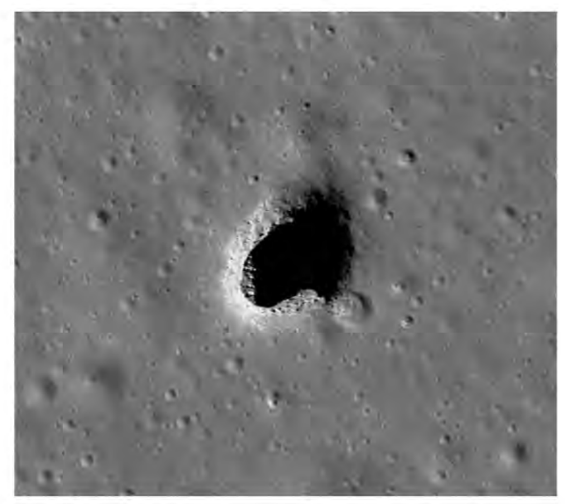

Figure 16. An image from the SELENE camera, hypothesized to be a lava pit (Haruyama et al. 2009) in the Marius Hills shows similar morphology to spatter features formed over lava tubes.

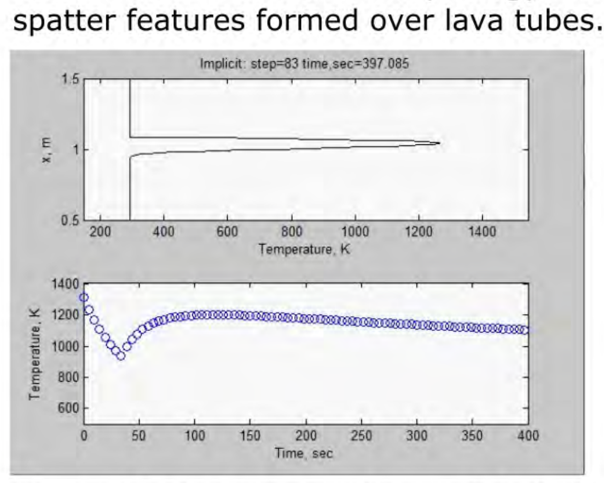

Figure 17. A heat transfer model shows the temperature profile though an accumulating spatter pile in the top window and a cooling curve of a single spot between two clasts. This model can be adjusted for lunar parameters and shows how accumulation affects cooling.

Can we apply this to the Moon?

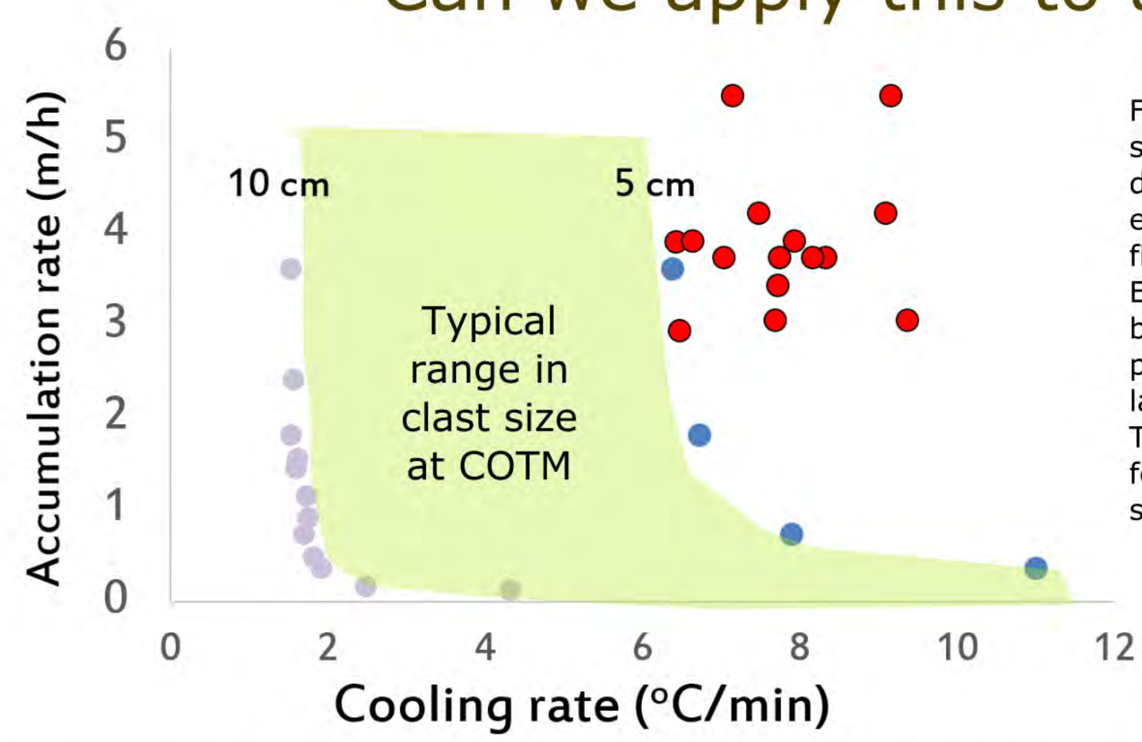

Figure 19. Modeled cooling rates of 5 cm thick spatter clasts (blue dots) and 10 cm clasts (grey dots) in Earth's atmosphere are lower than experimental cooling rates (red dots). The green field covers the size of spatter clasts seen at COTM. Experiments are likely cooling faster than predicted because the effect of heat loss from the side of the pile. Lunar spatter will likely cool slower due to the lack of heat loss by forced convection in a vacuum. The next goal for this project is to adjust the model for lunar conditions including the heat transfer specifics mentioned above and reduce gravity.

Acknowledgements: The production of this poster and travel for the author was provided by the NASA Postdoctoral Program, administrated by Universities Space Research Association.

References:

Haruyama, J., Hioki, K., Shirao, M., Morota, T., Hiesinger, H., van der Bogert, C. H., ... & Matsunaga, T. (2009). Possible lunar lava tube skylight observed by SELENE cameras. Geophysical Research Letters, 36(21).

Hughes, S. S., Smith, R. P., Hackett, W. R., & Anderson, S. R. (1999). Mafic volcanism and environmental geology of the eastern Snake River Plain, Idaho. Guidebook to the geology of eastern Idaho: Idaho Museum of Natural History, 143-168.

Kuntz, M. A., Spiker, E. C., Rubin, M., Champion, D. E., & Lefebvre, R. H. (1986). Radiocarbon studies of latest Pleistocene and Holocene lava flows of the Snake River Plain, Idaho: Data, lessons, interpretations. Quaternary Research, 25(2), 163-176.

Sumner, J. M. (1998). Formation of clastogenic lava flows during fissure eruption and scoria cone collapse: the 1986 eruption of Izu-Oshima Volcano, eastern Japan. Bulletin of Volcanology, 60 (3), 195-212.